Technical University of Denmark

DTU

Development and interaction of rotor wakes

Sørensen, Jens Nørkær; Mikkelsen, Robert Flemming; Kabardin, I K; Litvinov, I V; Naumov, I V; Okulov, Valery

Link back to DTU Orbit

DTU Library
Technical Information Center of Denmark

PAPER • OPEN ACCESS

Development and interaction of rotor wakes

To cite this article: J N Sørensen *et al* 2018 *J. Phys.: Conf. Ser.* **1037** 072045

View the article online for updates and enhancements.

Related content

- Wake developments behind different configurations of passive disks and active rotors
  V L Okulov, I V Litvinov, R F Mikkelsen et al.

- An influence of the different incoming wake-like flows on the rotor vibrations
  I V Naumov, I K Kabardin, R F Mikkelsen et al.

- Impact of Complex Orography on Wake Development: Simulation Results for the Planned WindForS Test Site
  Thorsten Lutz, Christoph Schulz, Patrick Letzgus et al.

Development and interaction of rotor wakes

J N Sørensen[1]**, R F Mikkelsen**[1]**, I K Kabardin**[2]**, I V Litvinov**[2]**, I V Naumov**[2]**,
V L Okulov** [1,2]

[1]Department of Wind Energy, Technical University of Denmark, 2800 Lyngby,
Denmark
[2] Kutateladze Institute of Thermophysics, SB RAS, Novosibirsk 630090, Russia

E-mail: jnso@dtu.dk

Abstract. The present work shows the results of a series of experimental investigations of the wake development behind a model rotor subject to upstream disturbances created either by another rotor or by a disk. The experiments are carried out in a water flume in order to control the flow and to carry out visualizations and to perform optical diagnostics. The aim of the work is to clarify similarities and differences in the wake of a wind turbine subject to different inflow disturbances, and in particular to see if there is any difference in the rotor wake resulting from a upstream disturbance created by a rotor and one created by an immobile disk. The background for the study is an on-going discussion if disks can replace rotors in laboratory experiments. In the paper, we will also show new experimental data that support our main conclusion, which is that strong differences exist between the near wakes characteristics of a rotor and a disk.

Keywords: bluff-body and rotor aerodynamics, near and far wake, pair interactions, dual disks, dual rotors.

1. Introduction

There is an increasing interest in studying rotor wakes and interaction of rotor wakes of wind turbines in wind farms [1-2]. The distance between wind turbines typically ranges from 3 to 10 rotor diameters. Various engineering models for determining the available power of wind turbines located in wind farms have been proposed exploiting the conservation laws of the flow characteristics [3-5], and the influence of the ambient turbulence on the power characteristics has been investigated using numerical simulations [6]. In spite of the many theoretical and numerical investigations, there is a lack of experiments testing systematically the mutual influence between the turbines and their wakes. Experimental data is very complicated to obtain for natural atmospheric conditions due to the difficulty of performing controlled field experiments. In this regard, laboratory experiments using small models of the rotors operating in wind tunnels [2, 7-9] or water flumes [10, 11] have become an important alternative to field measurements. In some cases, for simplification, the rotating blades of the rotors have been replaced by solid or porous immobile disks [12, 13].

The present work concerns the assessment of the impact of different incoming flow conditions and flow disturbances on the behavior of single rotors or clusters of rotor. The experiments are carried out

in a water flume in order to control the flow and to carry out visualizations and optical measurements diagnostics. The aim of the work is to clarify similarities and differences in the wake of a wind turbine subject to different inflow disturbances, and in particular to see if there is any difference in the rotor wake resulting from a upstream disturbance created by a rotor and one created by an immobile disk.

2. Experimental Method and Results

The experiments are carried out in a water flume of length 35m, 3m width and an operative height of 0.9m. The 3m wide test section is fitted with transparent walls at a distance of 20 m from the channel inlet. The free flow speed in the flume was U = 0.6 m/s. A Plexiglas disk (not perforated) of diameter D = 300 mm was used as passive wake generator (denoted Disk in the following), and the active wake generator (denoted Rotor in the following) was represented by a three-bladed rotor model of diameter D = 376 mm, corresponding to those used in previous works on disk and rotor far wakes [14-18]. The disk and rotor were chosen with different diameters because the main frequency (0.27 Hz and 0.28 Hz, respectively) and amplitude of pulsations gave almost the same values in the far wake. The Reynolds number based on rotor diameter and the initial flow in the flume varies in the range 140.000 < Re < 240.000 [15]. The velocity fields were measured with a Dantec stereo PIV system in a 3-D configuration with a camera placed in front of the flume and the illumination cross-section in the *x-y* plane. The light source of the PIV light sheet was a Nd:YAG pulse laser with 532 nm wavelength. The images were recorded with a Dantec HiSense II camera with a focal distance of 55 mm and pixel resolution. The area of the PIV study of the wakes was divided into a series of measurement windows. The windows were 532x356 mm with 40 mm overlap to ensure to cover the entire velocity field. Every measurement window was positioned in the same place of the test transparent section. The wake distance from the setup to the testing section was changed by translating a movable platform along the flume axis *x*.
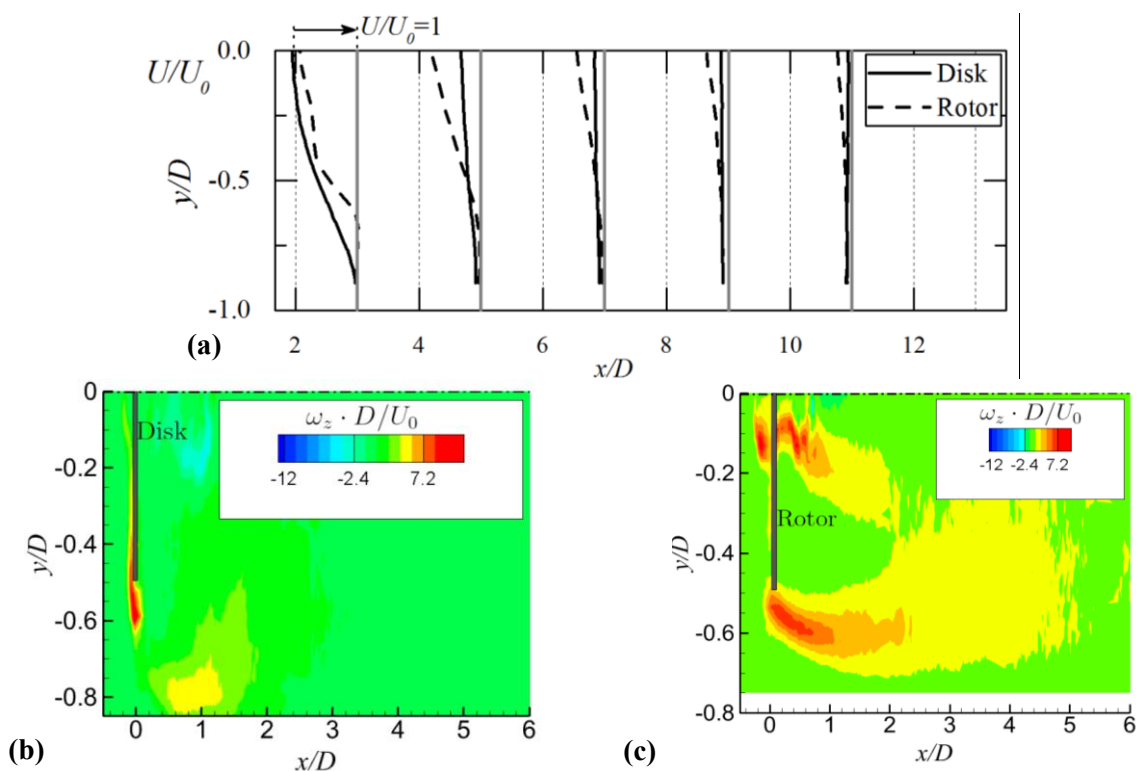

Figure 1. (a) Comparisons of velocity profiles U/U_0 in half-wake behind a disk and a rotor. Azimuthal vorticity distributions in a longitudinal section of **(b)** the disk half-wake and **(c)** the rotor half-wake.

The development of the average axial velocity profiles is in fig. 1a compared at different downstream cross-sections, showing the initial development of the wakes up to 10D downstream. The comparison shows the existence of a strong wake just behind the cross-section of the disk, resulting ultimately in a complete stop of the flow behind the disk. At the downstream cross-sections, it can be observed that the rotor wake recovers slower than the wake of the disc. This fact is in agreement with previous investigations [19-20]. The strengths of the two wakes differ because the deficit of the axial velocity in the near wake of the rotor, here up to 6D, is still influenced by the azimuthal vorticity originating from the tip vortices behind the rotor (fig. 1c), whereas this is absent behind the disk (fig. 1b). In fig. 2 we depict the turbulence levels generated by the upstream located Disk (D) (fig. 2a) and the Rotor (R) (fig. 2b) at different downstream locations. As seen from the figures, the turbulence levels are largely similar.
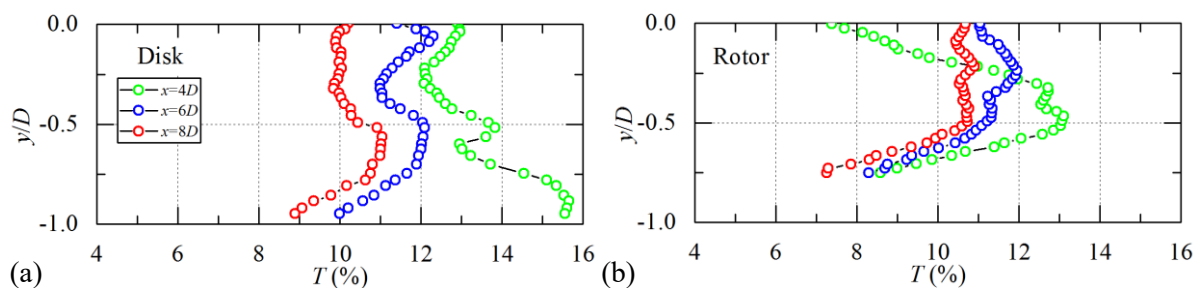

Figure 2. Turbulence levels behind the 'turbulence generators':
(a) Disk and (b) Rotor in three different cross-sections (4*D*, 6*D*, 8*D*).

It is also interesting to compare the performance of the test rotor subject to different upstream devises (Rotor or Disc) as function of the distance between the test rotor and the upstream device. This is achieved by measuring rotor torque and thrust by strain gauges installed in the rotor mounting [15, 25]. The voltage of the sensors was amplified by a preamplifier Scout 55, produced by Hootinger Baldwin Messtechnik, and was digitized by the ADC produced by National Instruments Company. Both strain sensors were calibrated with an inaccuracy of less than one percent using reference weights. The power and thrust coefficients of the test rotor are shown in fig. 3 and in table 1. The power and thrust coefficients of the test rotor subject to the inflow of the upstream located Disk are referred to as C_{PD} and C_{TD}, respectively, and the power and thrust coefficients subject to the inflow of the upstream located Rotor are denoted C_{PR} and C_{TR}, respectively.
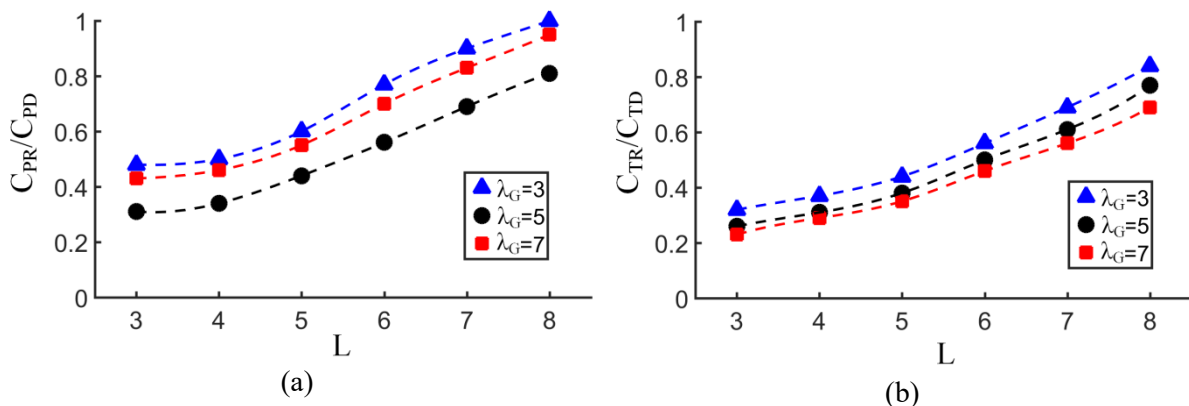

Figure 3. The ratio of power coefficients C_{PR} to C_{PD} (a) and the ratio of thrust coefficients C_{TR} to C_{TD} (b) as function of different distances, *L*, from the (D) and (R) wake generators of the testing rotor at λ=5.

The measured data serves to calculate average values of the torque and thrust acting on the axis of the test rotor. This system recorded the electrical signal of the strain sensors with a frequency of 120 Hz for 60 s [15, 25]. The test rotor, which was placed at various distances of $L = 3 - 8D$ downstream of the (D) and (R) generators, was operated optimally at a tip speed ratio $\lambda = 5$. Furthermore, three different wakes were tested behind the (R) generator operated at tip speed ratios $\lambda_G = 3$, 5 (optimal) and 7. The ratios of all power coefficients C_{PR} in the Rotor -wakes to the C_{PD} in the disk wake for different values of L and λ_G are shown in figure 3a, and the corresponding ratio of thrust coefficients C_{TR} to C_{TD} are depicted in figure 3b. The power and thrust of the test rotor in the Rotor-wake takes lower values than in the Disk-wake, which coincide with the behavior of the velocity deficit of the Disk and Rotor wakes on fig. 1a. For all distances, L, the power in the Rotor-wake generating at the optimal regime with $\lambda_G = 5$ corresponds to a minimum, whereas all thrusts grows with λ_G. The first point shows the possibility of reaching a maximum for the performance of an array of turbines operating at non-optimal conditions. The difference in the power and thrust in both (D) and (R) wakes dies out at increasing distances L when the deficits become small (fig. 1a).

Table 1. Values of coefficient C_{PR} and C_{TR} at $\lambda = 5$ and different values of λ_G and values of C_{PD} and C_{PD}

	L							L					
	3	4	5	6	7	8		3	4	5	6	7	8
C_{PR}, $\lambda_G=3$	0.48	0.50	0.60	0.77	0.90	1.00	C_{TR}, $\lambda_G=3$	0.07	0.11	0.21	0.24	0.26	0.28
C_{PR}, $\lambda_G=5$	0.31	0.34	0.44	0.56	0.69	0.81	C_{TR}, $\lambda_G=5$	0.07	0.11	0.23	0.27	0.28	0.29
C_{PR}, $\lambda_G=7$	0.43	0.46	0.55	0.70	0.83	0.95	C_{TR}, $\lambda_G=7$	0.09	0.14	0.28	0.34	0.36	0.39
C_{PD}	0.14	0.19	0.22	0.27	0.29	0.32	C_{TD}	0.52	0.62	0.76	0.81	0.80	0.79

Next, the kinematic characteristics of the wake behind the test rotors for the (D) and (R) cases will be analyzed to predict the properties of a next downstream turbine (third element on the rotor array), because in our early investigation it was found that a simple dual disk-disk system could not adequately represent the velocity in the wake behind a rotor-rotor system [14, 16]. This was explained by the strong difference in the kinematic characteristics of the two systems. In both cases of (D) and (R) wake generators, just like in the uniform flow [18], the same self-similar solution of the far wakes are found with the rate "-2/3", with closing factors 0.51 and 0.71 (fig. 4a and 4c), behind the test rotor located in the wakes with high turbulent oscillation levels (fig. 2). The next plots (fig. 4b and 4d) also show good correlations between the velocity profiles at the distances $L=2-10D$ where the third element (rotor) can be placed in accordance with a typical distance between turbines in ordinary wind farms. It is clearly seen that the difference in the profiles at a distance more than 3D is limited, indicating that the test rotor can restructure the initial differences in the Disk and the Rotor wake to very similar forms. The turbulence levels in the wakes behind the test rotor (fig. 5) also shows an insignificance difference between the (D) and (R) cases.
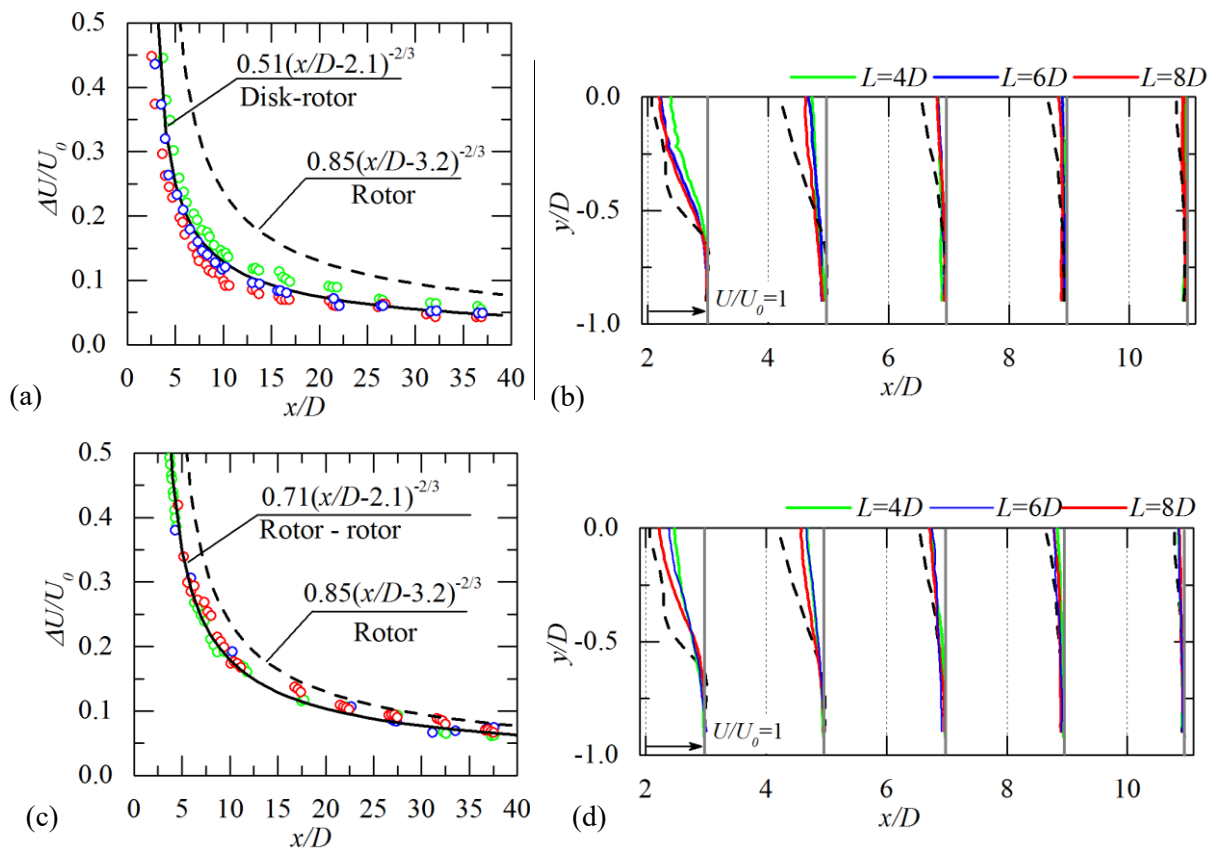
Figure 4. Development of the deficit velocity in the wakes behind the test rotor subject to a turbulent inflow generated by the wake generators (D) (a and b) and (R) (c and d). The deficit reductions with the rate "-2/3" are in the far wake behind the test rotors located in turbulent wake flows shown by solid lines (-) ; and the one for a rotor in initial uniform flow is shown by dashed lines (- -); (b and d) velocity profiles, U/U_0, at different distance $x = 2\text{-}10D$ behind the test rotor, with different line-colors indicating the distance L from the generators to test rotor.

The velocity profiles and turbulence levels of both systems with the initial (D) and (R) generators (fig. 4, 5) can produce wakes with more similar kinematic characteristics than for the two-different dual systems, i.e. disk-disk or rotor-rotor [14, 16].

So, there is a possibility to use upstream wake disturbances generated both by a Disk and by a Rotor to get similar velocity profiles and turbulence levels behind the second element, i.e. the test rotor, and achieving small differences in the power production by the third element (rotor) in this array.
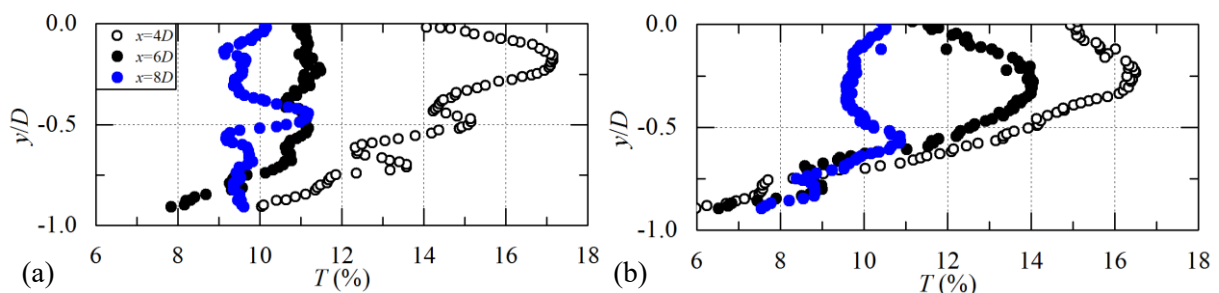

Figure 5. Turbulence levels in the wakes behind testing rotor at the cross-sections (x/D=4, 6, 8) with two different initial disturbances generated by upstream (L_x=6D) (D) (a) or (R)(b).

3. Conclusions

In the current investigation, the influence of two different initial wakes generated by a disk and a rotor, respectively, were investigated. The strong difference in the development of the initial wakes behind an immobile disk and an operating rotor was found by PIV-measurements and explained by different types of vorticity fields being generated. The self-similarity behavior of the rotor far-wake with the decay rates: "-2/3" of the deficit-velocity reduction and "1/3" of the wake expansion was again confirmed behind a test rotor subject to different incoming wakes with strong turbulence levels (up to 20%).

The results did not support alternative wake developments, which has suggested different decay rate values, such as "-2" for changes of the velocity deficit and "1" for the wake expansion [21-23]. Indeed disk and rotor far wakes with decay rates "-2/3" correspond to the well-known classical solution for the development of turbulent far wakes behind axisymmetric bluff bodies [24], which has been well reproduced in wind tunnels and water flumes at large Reynolds numbers. Indeed, in accordance with [24], the second solution has only been truly observed in very long time DNS simulations of time-dependent wakes.

It was found that a rotor wake generated at optimum operating conditions, results in a minimum power production of the test rotor. This indicates the possibility of enhancing the overall performance of the second rotor by letting the first rotor operate at a non-optimal tip speed ratio. For both Disk and Rotor initial disturbance elements, the wake behind the second test rotor consists of similar velocity profiles and turbulence levels, which shows that the differences in the wake generated by an upstream disk and an upstream rotor have a limited impact on the far wake behind the subsequent wind turbines. Therefore, as an overall conclusion, discs can be used to replace rotors when carrying out wind farm experiments, but they should not be placed in front of the rotor being tested. Hence testing a third rotor in a row, a D-R configuration can be utilized upstream of the rotor, whereas the configurations D-D and R-D will not work properly.

References

[1] Adaramola M. S., Krogstad P.-Å. Experimental Investigation of Wake Effects on Wind Turbine Performance. Renewable Energy, 2011; 36, 2078–2086.

[2] Subramanian, B., Chokani, N., Abhari, R. S. Aerodynamics of wind turbine wakes in flat and complex terrains. Renewable Energy, 2015: 85: 454-463. DOI: 0.1016/j.renene.2015.06.060.

[3] Herp, J., Poulsen, U.V., Greiner, M. Wind farm power optimization including flow variability. Renewable Energy, 2015: 81: 173-181 DOI: 10.1016/j.renene.2015.03.034.

[4] Abdulrahman M., Wood D. Some Effects of Efficiency on Wind Turbine Interference and Maximum Power Production. Wind Engineering Vol 39, Issue 5, pp. 495 - 505 10.1260/0309-524X.39.5.495 .

[5] Nygaard N.G. Wakes in very large wind farms and the effect of neighbouring wind farms // Journal of Physics: Conference Series. – 2014. – T. 524. – C. 012162

[6] Breton SP, Nilsson K, Olivares-Espinosa H, Masson C, Dufresne L, Ivanell S. Study of the influence of imposed turbulence on the asymptotic wake deficit in a very long line of wind turbines. *Renewable Energy* 2014; 70: 153-163.

[7] Dufresne NP, Wosnik M. Velocity Deficit and Swirl in the Turbulent Wake of a Wind Turbine. J. Marine Technology Society 2013; 47(4): 193-205.

[8] Bartl J, Pierella F, Sætran L. Wake measurements behind an array of two model wind turbines. Energy Procedia 2012; 24:305-312.

[9] Rockel S., Peinke J., Holling M., Cal R.B. Wake to wake interaction of floating wind turbine models in free pitch motion: An eddy viscosity and mixing length approach. Renewable Energy 2016: 85: 666-676.

[10] Chamorro, L. P., Hill, C., Morton, S., Ellis, C., Arndt, R. E. A., Sotiropoulos, F. On the interaction between a turbulent open channel flow and an axial-flow turbine.J. Fluid Mech. 2013: 716, 658–670.

[11] Okulov VL, Naumov IV, Mikkelsen RF, Kabardin IK, Sørensen JN. A regular Strouhal number for large-scale instability in the far wake of a rotor. *J. Fluid Mech.* 2014; 747: 369-380.

[12] Lignarolo LEM, Ragni D, Ferreira CJ, Van Bussel GJW Experimental comparison of a wind-turbine and of an actuator-disk near wake. Journal of Renewable and Sustainable Energy 2016: 8(2): 023301.

[13] Muller Y.A., Aubrun S., Masson C. Determination of real time predictors of the wind turbine wake meandering. Exp Fluids (2015) 56:53 DOI 10.1007/s00348-015-1923-9.

[14] Okulov V L, Mikkelsen R F, Naumov I V, Litvinov I V, Gesheva E, Sørensen J N 'Comparison of the far wake behind dual rotor and dual disk configurations' Journal of Physics: Conference Series 753 (2016) 032060. doi:10.1088/1742-6596/753/3/032060.

[15] Naumov I.V., Kabardin I.K., Mikkelsen R.F., Okulov V.L., Sørensen J.N. An influence of the different incoming wake-like flows on the rotor vibrations. Journal of Physics: Conf. Series. 2017. vol. 854, p. 012034.

[16] Okulov V L, Litvinov I V, Mikkelsen R F, Naumov I V, Sørensen J N ' Wake developments behind different configurations of passive disks and active rotors '. Journal of Physics: Conference Series. IOP Publishing, 2017. vol. 854, p. 012035.

[17] Litvinov I.V., Naumov I.V., Okulov V.L., Mikkelsen R.F. Comparison of far wake behind solid disk and three-blade rotor. *Journal of Flow Visualization and Image Processing* 2015: 22(4): 175-183.

[18] Okulov VL, Naumov IV, Mikkelsen RF, Sørensen JN. Wake effect on a uniform flow behind wind-turbine model. *J. of Physics: Conference series.* 2015; 625: 012011.

[19] Kuik GAM van, Sørensen JN, Okulov VL. The rotor theories by Professor Joukowsky: Momentum Theories. Prog Aerospace Sci 2015; 73: 1-18. DOI: 10.1016/j.paerosci.2014.10.

[20] Okulov VL, Sørensen JN, Wood DH. The rotor theories by Professor Joukowsky: Vortex Theories. Prog Aerospace Sci 2015; 73: 19-46. DOI: 10.1016/j.paerosci.2014.10.002.

[21] Lissaman PBS. Energy effectiveness of arbitrary arrays of wind turbines. In: AIAA Paper 79-0114, 1979. p. 1–7.

[22] Jensen N. A note on wind turbine interaction. Technical report Ris-M-2411. Roskilde, Denmark: Risø National Laboratory; 1983.

[23] Bastankhan M, Porte-Agel F. A new analytical model for wind turbine wakes. Renewable Energy 2014; 70: 116-123.

[24] George W.K. Asymptotic Effect of Initial and Upstream Conditions on Turbulence. J. Fluids Eng 2012; 134(6), 061203.

[25] Naumov I.V., Kabardin I.K., Mikkelsen R.F., Okulov V.L., Sørensen J.N. Performance and wake conditions of a rotor located in the wake of an obstacle. Journal of Physics Conference Series. 2016. vol. 753, p. 032051.